Improving GAN Equilibrium by Raising Spatial Awareness

Jianyuan Wang[1,2]   Ceyuan Yang[1]   Yinghao Xu[1]   Yujun Shen[1]   Hongdong Li[2]   Bolei Zhou[3]

[1]The Chinese University of Hong Kong   [2]The Australian National University

[3]University of California, Los Angeles

Abstract

The success of Generative Adversarial Networks (GANs) is largely built upon the adversarial training between a generator (G) and a discriminator (D). They are expected to reach a certain equilibrium where D cannot distinguish the generated images from the real ones. However, such an equilibrium is rarely achieved in practical GAN training, instead, D almost always surpasses G. We attribute one of its sources to the information asymmetry between D and G. We observe that D learns its own visual attention when determining whether an image is real or fake, but G has no explicit clue on which regions to focus on for a particular synthesis. To alleviate the issue of D dominating the competition in GANs, we aim to raise the spatial awareness of G. Randomly sampled multi-level heatmaps are encoded into the intermediate layers of G as an inductive bias. Thus G can purposefully improve the synthesis of certain image regions. We further propose to align the spatial awareness of G with the attention map induced from D. Through this way we effectively lessen the information gap between D and G. Extensive results show that our method pushes the two-player game in GANs closer to the equilibrium, leading to a better synthesis performance. As a byproduct, the introduced spatial awareness facilitates interactive editing over the output synthesis. Demo video and code are available at https://genforce.github.io/eqgan-sa/.

1. Introduction

Generative Adversarial Network (GAN) has made huge progress toward image synthesis [4, 13, 22, 23, 28]. GAN is formulated as a two-player game between a generator (G) and a discriminator (D) [13], where G targets at reproducing the distribution of observed data through synthesizing new samples, and D competes with G by distinguishing the generated images from the real ones. In principle, they are expected to reach an equilibrium where D cannot tell the real and fake images apart [2, 13].

In practice, it turns out to be difficult to achieve such an equilibrium when training modern GAN variants [4,
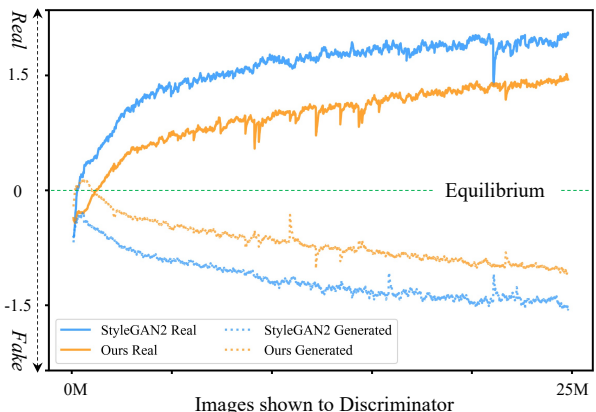

Figure 1. **Discriminator's output scores for real and generated samples during training.** A higher number indicates more realistic. We use StyleGAN2 [23] as the baseline and implement the proposed method over it on the LSUN Cat dataset. For a clear comparison, we report the minimum of the scores for real samples and the maximum for generated samples, which are supposed to be close to each other. However, the curve for the real is always above the curve for the generated. Our method can reduce the gap toward the equilibrium as well as improve the synthesis quality.

21–23], despite their appealing synthesis quality. Taking StyleGAN2 [23] as an example, D almost always assigns a higher score to real images than to fake ones throughout the *entire* training process, as the blue lines shown in Fig. 1. It suggests that D can easily beat G in the competition. Increasing the model capacity of G barely helps mitigate this issue [4]. From this point of view, we can hold that G fails to fool D even after the model converges, leaving a gap between the real and synthesized distributions. Such a disequilibrium remains much less explored in recent years, in spite of the rapid development of new GAN models.

To investigate the source of the aforementioned disequilibrium, we analyze the behaviour of D to figure out its advantage over G. With the help of GradCAM [30] as a neural network interpretation tool, we visualize the intermediate feature maps produced by D. As shown in Fig. 2, given a target image, either real or generated, D holds its own visual attention, even it is *merely* learned
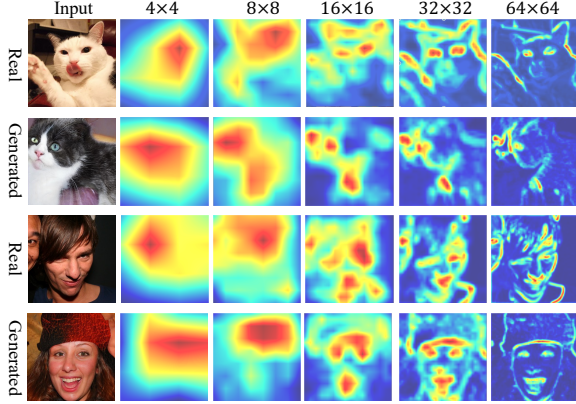
Figure 2. **Spatial visual attention at the intermediate layers of the discriminator,** visualized by GradCAM. A bright color indicates a strong contribution to the final score. '64 × 64' indicates being upsampled from a 64×64 feature map. The samples are the real images and the images generated by StyleGAN2 [23].

from a bi-classification task (*i.e.*, differentiating the real and fake domains). In other words, D is aware of which flawed regions to pay attention to when making the real/fake decision. Such an attentive property eases its competition to G because D can simply focus on the regions that are poorly synthesized by G. On the contrary, to produce an image, G takes a randomly sampled latent code as the input and has no explicit clue about which regions to focus on, let alone knowing the spatial preference of D. Due to such an information asymmetry, G may omit some important cues picked by D and hence get defeated in the two-player game.

In this paper, we propose a training method, termed as **EqGAN-SA**, to improve the **Eq**uilibrium of **GAN** through raising **S**patial **A**wareness. Concretely, we strive to lessen the information asymmetry between G and D by raising the *spatial awareness* of G. We design a hierarchical heatmap sampling strategy to match the coarse-to-fine synthesis mechanism [22, 36]. The sampled multi-level heatmaps are integrated into the per-layer feature maps of G. Meanwhile, to make sure G utilize the input heatmap adequately, we involve D as a regularizer to spatially supervise the generation process, through aligning the spatial awareness of G with the visual attention induced from D.

We evaluate the proposed method on various datasets. As the orange lines shown in Fig. 1, we push the competition between G and D closer to the equilibrium compared to the baseline method [23]. Consequently, our EqGAN-SA learns a distribution that is more identical to the real one, leading to a substantial improvement in the synthesis performance. For example, with Fréchet Inception Distance (FID) [16] as the metric, we improve the baseline from 3.66 to 2.96 on FFHQ dataset [22] under 256×256 resolution. In addition, we can achieve interactive editing over the output image by altering the spatial heatmaps fed into G.

2. Analyzing GAN Equilibrium

Although GANs [2, 9, 13, 22, 23] are supposed to reach an equilibrium between G and D, this is barely fulfilled in practice. Typically, D wins over G most of the time. In this section, we attempt to investigate the cause of such a phenomenon. Sec. 2.1 briefly reviews the formulation of GANs and describes the disequilibrium between G and D. Sec. 2.2 interprets the visual attention learned by D, which could be one of the key sources for the disequilibrium.

2.1. Learning Objective of GAN

GAN training [13] is formulated as a two-player game, where a generator is trained to recover the real distribution p_r over data $\{\mathbf{x}\}$, while a discriminator is optimized to differentiate between p_r and the generated distribution p_g. The overall objective function is

$$\min_G \max_D V(D, G) = \mathbb{E}_{\mathbf{x} \sim p_r}[\log D(\mathbf{x})] \\ + \mathbb{E}_{\mathbf{z} \sim p_z}[\log(1 - D(G(\mathbf{z})))], \tag{1}$$

where $\mathbf{z}$ is a randomly sampled vector, subject to a prior distribution, p_z. In particular, Goodfellow *et al.* [13] point out that the minimax game defined by GAN will reach an equilibrium point, where G recovers the training data distribution while D fails to distinguish the real and fake distributions. In that case, D is supposed to assign same realness scores to the real and synthesized samples.

Observation of Disequilibrium. We observe that such an equilibrium is seldom achieved in most GAN variants [4, 22, 23]. It appears that D almost always dominates the G-D competition, assigning a higher score to real data. An example of training StyleGAN2 [23] on LSUN Cat [38] is shown in Fig. 1. We can spot an obvious gap even between D's minimum score for real images and the maximum score for synthesized images. Such a phenomenon implies that the generated distribution p_g is far from the real distribution p_r, affecting the synthesis quality.

2.2. Visual Attention of Discriminator

After observing the disequilibrium in the interplay between D and G, we would like to investigate the behavior of D to see how it manages to outperform G. Prior work on network interpretability, like CAM [40], has found that a classifier tends to focus on some discriminative regions to categorize a given image to the proper class. However, the discriminator in GANs is trained with the relatively weak supervision, *i.e.*, only having real or fake labels. Whether it can learn the attentive property from such a bi-classification task remains unknown. To look under the hood, we apply GradCAM [30] as an interpretability tool on the well-trained discriminator of StyleGAN2 [23].

Specifically, for a certain layer and a certain class, GradCAM calculates the importance weight of each neuron
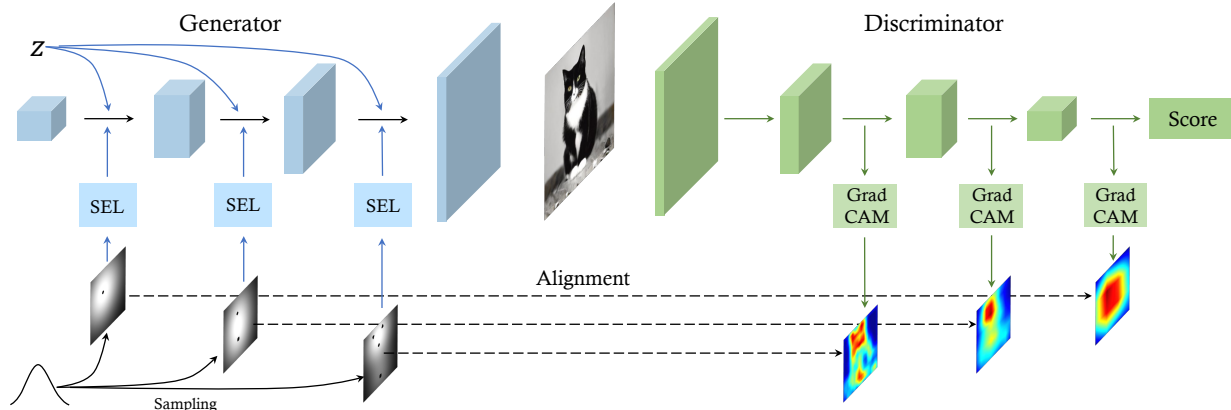
Figure 3. **Illustration of EqGAN-SA.** We conduct spatial encoding in G and align its spatial awareness with D attention maps. Specifically, we randomly sample spatial heatmaps and encode them into G via the spatial encoding layer (SEL). To implement the alignment during training, we calculate D attention maps over the generated samples via GradCAM.

by average-pooling the gradients back-propagated from the final classification score, over the width and height. It then computes the attention map as a weighted combination of the importance weight and the forward activation maps, followed by a ReLU [11] activation. The attention map has the same spatial shape as the corresponding feature map. In this work, we report the GradCAM attention maps all using gradients computed via maximizing the output of D. It reflects the spatial preference of D in making a 'real' decision. In practice we find the attention maps are almost the same if instead minimizing the output of D, which indicates the areas that largely contribute to the decision are the same for a discriminator, no matter positively or negatively. The region with higher response within the attention map contributes more to the decision.

Fig. 2 visualizes some GradCAM results under multiple feature resolutions. They are obtained from the discriminators of two StyleGAN2 models, trained on LSUN Cat and FFHQ respectively. We have following observations: (1) D learns its own visual attention on both real and generated images. It suggests that D makes the real/fake decision by paying more attention to some particular regions. (2) The visual attention emerging from D shows a hierarchical property. In the shallow layers (like 64×64 and 32×32 resolutions), D is attentive to local structures such as edge lines in the image. As the layer goes deeper, D progressively concentrates on the overall location of discriminative contents, $e.g.$, the face of a cat. (3) The hierarchical attention maps have fewer 'local peaks' at more abstract feature layers with a lower resolution. For example, there is only one peak in the 4×4 attention maps.

3. Improving GAN Equilibrium

As shown in Sec. 2, the discriminator of GANs has its own visual attention when determining real or fake image. However, when learning to transform a latent vector into a

realistic image, the generator receives no explicit clue about which regions to focus on. Specifically, for a particular synthesis, G has to decode all the needed information from the input latent code. Furthermore, G has no idea about the spatial preference of D on making the real/fake decisions. Such an information asymmetry puts G at a disadvantage when competing with D. In this section, we propose to raise the spatial awareness of G to lessen the information gap between G and D. The overall framework is illustrated in Fig. 3, which mainly consists of two steps, (1) explicitly encoding spatial awareness into G with a hierarchical heatmap sampling strategy and (2) aligning the spatial awareness of G with the visual attention from D via a feedback regularizer. Sec. 3.1 and Sec. 3.2 introduce these two techniques respectively.

3.1. Encoding Spatial Awareness in Generator

Hierarchical Heatmap Sampling. To improve the awareness of G on spatial regions, we propose a hierarchical heatmap sampling algorithm. This heatmap is responsible for teaching G which regions to pay more attention to. Inspired by the visual attention induced from D as in Sec. 2.2, we abstract our heatmap as a combination of several sub-regions and a background. Taking the heatmap at the 4×4 resolution as an example (leftest in Fig. 3), it tells G there is one region to focus on, whose center locates at the black dot. We formulate each sub-region as a 2D map, H_i, which is sampled subject to a Gaussian distribution

$$H_i \sim \mathcal{N}(\mathbf{c_i}, \mathbf{cov}), \tag{2}$$

where $\mathbf{c_i}$ and $\mathbf{cov}$ denote the mean and the covariance. According to the definition of 2D Gaussian distribution, $\mathbf{c_i}$ just represents the coordinates of the region center. The final heatmap can be written as the sum of all sub-maps, $H = \sum_{i=1}^{n} H_i$, where n denotes the total number of local regions for G to focus on.

3

As pointed out in the prior works [22, 36], the generator in GANs learns image synthesis in a coarse-to-fine manner, where the early layers provide a rough template and the latter layers refine the details. To match such a mechanism, we design a hierarchical heatmap sampling algorithm. Concretely, we first sample a spatial heatmap with Eq. (2) for the most abstract level (*i.e.*, with the lowest resolution), and derive the heatmaps for other resolutions based on the initial one. The number of centers, n, and the covariance, **cov**, adapt accordingly to the feature resolution.

Heatmap Encoding. We incorporate the spatial heatmaps into G to raise its spatial awareness. It generally can be conducted in two ways, via feature concatenation or feature normalization [18, 27]. We use a spatial encoding layer (SEL), respectively trying these two variants, denoted as SEL$_{concat}$ and SEL$_{norm}$. Specifically, inspired by SPADE [27], the variant SEL$_{norm}$ integrates the hierarchical heatmaps into the per-layer feature maps of G with normalization and denormalization operations, as

$$SEL_{norm}(F, H) = \phi_\sigma(H) \frac{F - \mu(F)}{\sigma(F)} + \phi_\mu(H), \quad (3)$$

where F denotes an intermediate feature map produced by G, which is with the same resolution as H. $\mu(\cdot)$ and $\sigma(\cdot)$ respectively stands for the functions of computing channel-wise mean and standard deviation. $\phi_\mu(\cdot)$ and $\phi_\sigma(\cdot)$ are two learnable functions, whose outputs are point-wise and with a shape of $(h, w, 1)$. Besides, as shown in Fig. 4, we use a residual connection to stabilize the intermediate features. If not particularly specified, this paper adopts the variant SEL$_{norm}$ since it shows a slightly better performance.

It is worth noting, although we learn the SEL$_{norm}$ architecture from SPADE [27], these two methods are clearly different since SPADE targets at synthesizing images based on a given semantic segmentation mask, whose training requires paired ground-truth data, while our model is trained with completely unlabeled data. Meanwhile, SEL$_{norm}$ is just a replaceable component of our approach.

3.2. Aligning Spatial Awareness with Discriminator

Encoding heatmaps into G can explicitly raise its spatial awareness, but it is not enough to make G competitive with D. The reason is that, D learns its own visual attention based on the semantically meaningful image contents, but the heatmaps fed into G are completely arbitrary. Without further guidance, how G is supposed to utilize the heatmaps is ambiguous. For example, G has no idea about "whether to pay *more* or *less* attention on the highlighted regions in the heatmap". To make the best usage of the introduced spatial awareness, we propose to involve D as a regularizer to supervise G, to properly leverage the spatial knowledge.

Specifically, at each optimization step of G, we use D to generate the visual attention map via GradCAM as a self-
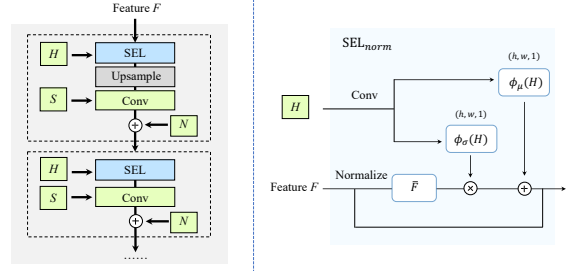

Figure 4. **Spatial Encoding Layer.** The left shows how the layer works over StyleGAN2 at each resolution, and the right describes the internal of the SEL$_{norm}$. The symbol 'S' represents the style in StyleGAN2, 'N' is the noise, and 'H' indicates the spatial heatmap. Learning from [27], we incorporate the spatial heatmaps into G via normalization and denormalization.

supervision signal. Besides competing with D, G is further trained to minimize the distance between the attention map induced from D and the input heatmap H. The loss function can be written as

$$\mathcal{L}_{align} = || \, \text{GradCAM}_D[G(H, \mathbf{z})] - H \, ||_1. \quad (4)$$

We truncate the $\mathcal{L}_{align}$ values if smaller than a constant τ, since the sampled heatmaps are not expected to perfectly match the real attention maps shaped by semantics. The threshold τ is set as 0.25 for all the experiments. Note that D is not updated in the process above and only used as a supervision signal to train G. Such a regularization loss aligns the spatial awareness of G with the spatial preference of D, narrowing the information gap between them.

4. Experiments

We evaluate the proposed EqGAN-SA on multiple benchmarks. Sec. 4.1 provides the implementation details. The main comparison and experimental results are presented in Sec. 4.2. Our EqGAN-SA could improve the spatial attentive property in G and mitigates the disequilibrium to some extent. Sec. 4.3 includes the comprehensive ablation studies on the role of each proposed component.

4.1. Implementation Details

Datasets. We conduct the experiments on the LSUN Cat [38], FFHQ [22], and LSUN Church [38] datasets. The LSUN Cat dataset contains $1600K$ real-world images regarding different cats. Following the setting of [21], we take $200K$ image samples from the LSUN Cat dataset for training. The FFHQ dataset consists of $70K$ high-resolution (1024×1024) images of human faces, under Creative Commons BY-NC-SA 4.0 license [33]. Usually, the images are horizontally flipped to double the size of training samples. The LSUN Church dataset includes $126K$ images with visually complex church scenes. It is worthy noting that all images are resized to 256×256 resolution.
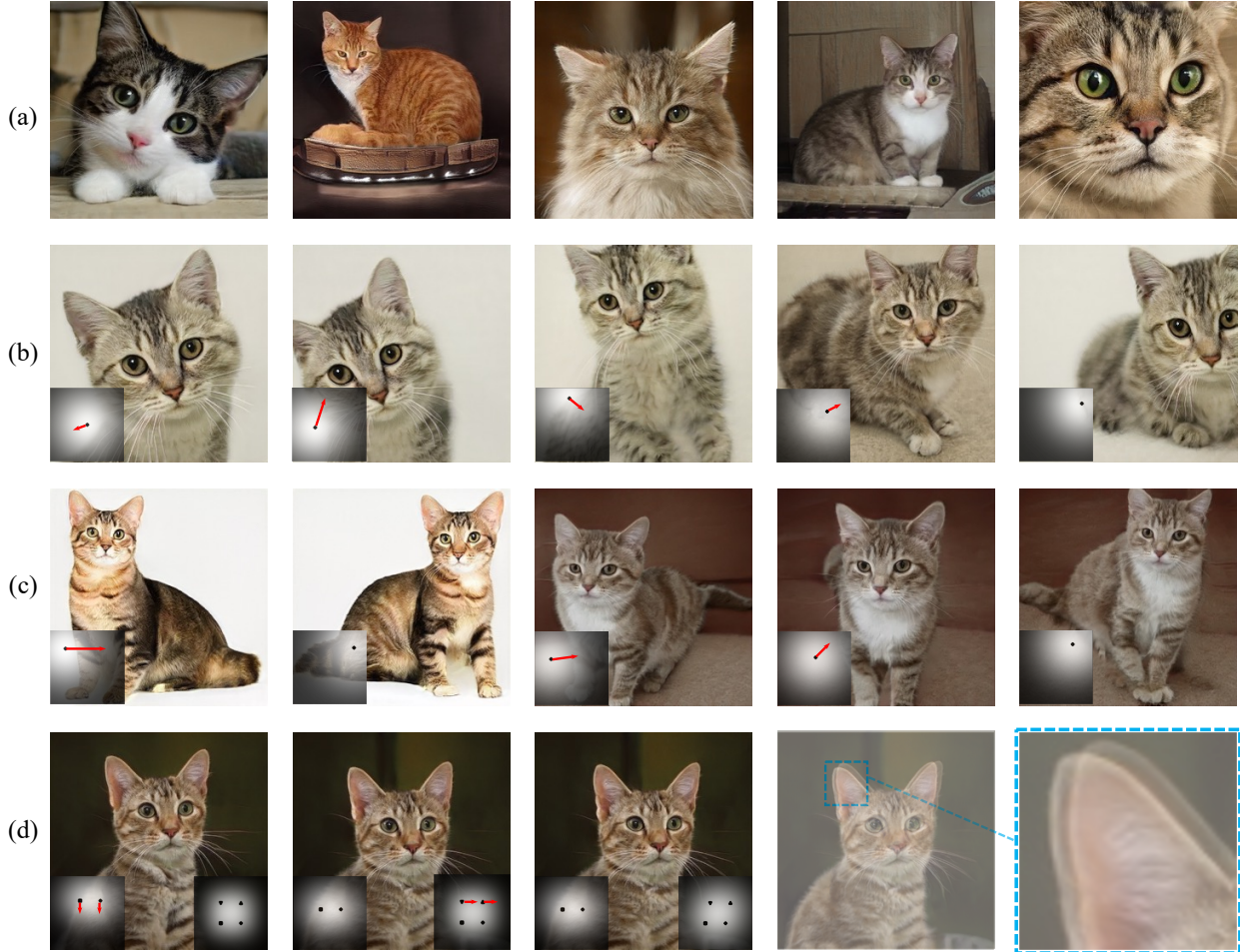
Figure 5. **Qualitative results on LSUN Cat dataset and the demonstration of spatial awareness via varying the spatial heatmaps of the generator.** Row (a) shows several generated samples of a model trained through EqGAN-SA. Rows (b) and (c) illustrate the spatial awareness of G: we keep the latent codes unchanged and move the spatial heatmap at the 4×4 level. The arrows indicate the movement direction, where the cat moves along with the varied heatmap. To further show the hierarchical structure, we move the heatmap at the finer level in the Row (d). Different from the body movement, the change in 8×8 heatmap (two centers) mainly moves the cat eyes, and the change in 16×16 heatmap (four centers) leads to subtle movement of the cat ears. It is worth noting that, as the content is being manipulated, our G knows to adjust the nearby regions to make everything coherent.

Spatial Heatmap Sampling and Encoding. In practice, we find the GradCAM maps on the fine resolutions are too sensitive to semantic cues. Therefore, we only conduct encoding on the level $0, 1, 2$ of G, *i.e.*, resolution 4×4, 8×8, and 16×16. We heuristically generate $1, 2, 4$ centers (in other words, sub-heatmaps) on these three levels. We sample the level 0 heatmap center $\mathbf{c_0^0}$ by a Gaussian distribution with a mean of $\left(\frac{h}{2}, \frac{w}{2}\right)$, and a standard deviation of $\left(\frac{h}{3}, \frac{w}{3}\right)$. To keep the heatmaps consistent at various levels, we sample the level $1, 2$ centers over the level 0 center. It indicates the mean of Gaussian distribution $\mathbf{c_n^1}$ and $\mathbf{c_n^2}$ is the sampled $\mathbf{c_0^0}$. Their standard deviations are $\left(\frac{h}{6}, \frac{w}{6}\right)$. If we shift the level 0 center, the heatmaps of other levels will move correspondingly. Following the coarse-to-fine manner, we decrease each center's influence area level by level. Besides, we drop the sampling if the level 0 center is outside the image. In our observation, the results of the proposed method are robust to these hyperparameters for heatmap sampling. Therefore, we use the same hyperparameters for heatmap sampling on all the datasets. More implementation details are provided in *Supplementary Material*.

Training. We implement our EqGAN-SA on the official implementation of StyleGAN2, such that the state-of-the-art image generation method StyleGAN2 [23] serves as our baseline. We follow the default training configuration of [21] for the convenience of reproducibility, and keep the hyperparameters unchanged to validate the effectiveness of our proposed framework. For example, we train all the models with a batch size of 64 on 8 GPUs and continue
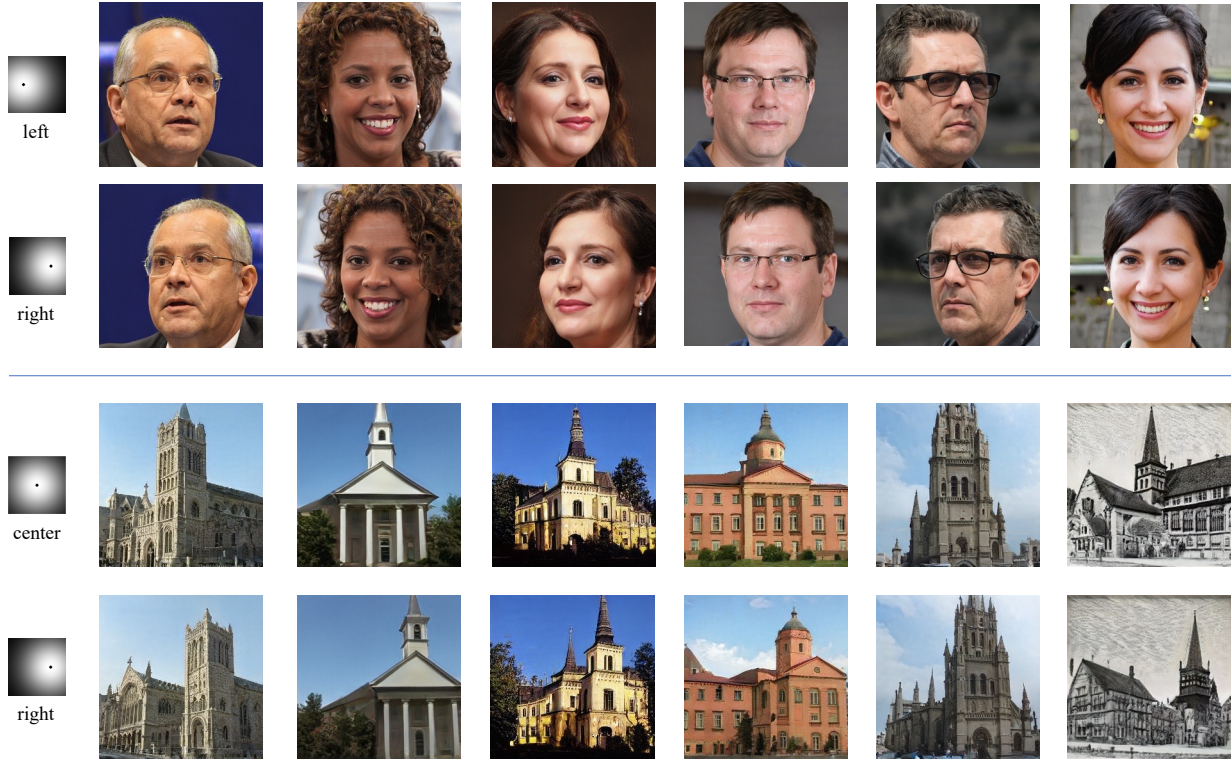
Figure 6. **Qualitative results on the FFHQ dataset (top) and the LSUN Church dataset (bottom)**. Each row uses the same spatial heatmap but different latent codes, and each column uses the same latent code. We can see that the spatial heatmap roughly controls the pose of the face and the viewpoint of the church building, which facilitates the interactive spatial editing of the output image.

the training until $25M$ images have been shown to the discriminator. Our method increases the training time by around 30% compared with the baseline.

Evaluation. We use Fréchet Inception Distance (FID) [16] between $50K$ generated samples and all the available real samples as the image generation quality indicator. We utilize a specific approximation of Wasserstein distance to quantify the degree of disequilibrium, *i.e.*, the distance between (a) the minimum discriminator scores for real samples and (b) the maximum scores for generated samples. We term it as Disequilibrium Indicator (DI), where DI $= \min(s_r) - \max(s_g)$. It indicates if D can distinguish between the hardest real image and most realistic generated image. To keep the result stable, we compute DI over 128 randomly sampled images (64 real and 64 fake) for 200 times and take the mean value. We also discuss the validity of DI in *Supplementary Material*.

4.2. Main Results

Spatial Awareness is Raised in Generator. As discussed in Sec. 3.1, we propose to encode spatial awareness into G. Here we provide the qualitative results in Fig. 5 and Fig. 6 to verify that G indeed learns to focus on the regions specified by input heatmaps. Specifically, we keep the latent vector unchanged and move the spatial heatmaps. As we

move the level 0 heatmap of the sample (b) and (c) in Fig. 5, the cat bodies move under the guidance of heatmap movement (indicated by red arrows). We can observe the same phenomenon by watching each column of Fig. 6. Furthermore, as illustrated by each row of Fig. 6, the human images generated with the same heatmap will put faces on the same location. In addition, as desired by our hierarchical design, moving level 1 and 2 heatmaps would affect local structures. For example, in the sample (d) of Fig. 5, the change in level 1 heatmap leads to a movement in cat eyes. As we slightly push the top two centers of level 2 heatmap to the right, the cat ears subtly turn right while other parts, even the cat whiskers, remain unchanged. These verify the effect of our hierarchical spatial encoding. We also notice G could adaptively modify the nearby texture and structure to give a reasonable image. Additionally, we visualize the generator intermediate features to investigate whether it has spatial awareness and the effect of our method, as shown in *Supplementary Material*. Overall, the moved contents depict the spatial awareness of G, which shows a hierarchical style and matches our design target.

Equilibrium is Improved. The quantitative results on the three datasets are provided in Tab. 1. On all the datasets, the metric DI shows a drop after encoding spatial awareness into G, and a further decrease with the help of

Table 1. **Quantitative results on LSUN Cat, FFHQ, and LSUN Church datasets, all trained with 25M images shown to discriminator.** The baseline uses the architecture of StyleGAN2 [22]. We use FID as the metric for image generation quality. We also formulate a metric Disequilibrium Indicator (DI), a specific form of Wasserstein distance [2], to quantify the disequilibrium. DI is calculated as $\min(s_r) - \max(s_g)$, where s indicates the discriminator outputs before the activation. We discuss the validity of DI and include the results of other metrics in *Supplementary Material*. $\downarrow$ denotes smaller is better.

Method	Cat [38] 256 × 256		FFHQ [22] 256 × 256		Church [22] 256 × 256	
	FID $\downarrow$	DI $\downarrow$	FID $\downarrow$	DI $\downarrow$	FID $\downarrow$	DI $\downarrow$
Baseline	8.36	3.64	3.66	1.62	3.73	3.01
+ SEL	7.82	3.12	3.39	1.38	3.55	2.59
+ $\mathcal{L}_{align}$	**6.81**	**2.39**	**2.96**	**0.73**	**3.11**	**2.07**

$\mathcal{L}_{align}$. For example, DI reduces from 3.64 to 3.12 and finally 2.39 on the LSUN Cat dataset. This observation verifies the hypothesis that the aforementioned information asymmetry is a source of GAN disequilibrium, and our proposed approach can mitigate the imbalance.

With the improved equilibrium, the image synthesis quality also becomes better. We observe that there are consistent improvements over the FID on three datasets, outperforming the baseline StyleGAN2. We also validate our idea on the basis of SN-DCGAN (DCGAN [28] with spectral normalization [25]) on the CIFAR-10 [24] dataset, as shown in Tab. 2.

4.3. Ablation Study

How Important is the Type of Spatial Heatmap Sampling? Different sampling strategies are applied here to validate our choice, as provided in Tab. 3. Specifically, 2D Gaussian noise is first considered as a straightforward baseline experiment since it provides non-structured spatial information. Accordingly, 2D Gaussian noise introduces no performance gains. It indicates, merely feeding a 2D heatmap but without any region to be emphasized is insufficient to raise spatial awareness and mitigate the disequilibrium.

Besides, we also use multiple-resolution spatial heatmaps but discard the hierarchical constraint, referred as Non-Hie in Tab. 3. Namely, spatial heatmaps at different resolutions are independently sampled. Obviously, the baseline is improved by this non-hierarchical spatial heatmap, demonstrating the effectiveness of the spatial awareness of G. Moreover, when the hierarchical sampling is adopted, we observe further improvements over the synthesis quality and equilibrium.

How Important is the Way of Spatial Encoding? In order to raise the spatial awareness of G, there exist several alternatives to implement. Therefore, we conduct

Table 2. **Quantitative results on the CIFAR-10 dataset over the baseline SN-DCGAN,** with conditional or unconditional image synthesis.

Method	Unconditional		Conditional	
	FID $\downarrow$	DI $\downarrow$	FID $\downarrow$	DI $\downarrow$
SN-DCGAN	23.72	1.85	19.89	1.61
+ Ours	**16.93**	**0.96**	**13.56**	**0.78**

Table 3. **Spatial Heatmap Sampling.** With other parts unchanged, we separately throw random Gaussian noise, spatial heatmap without hierarchical sampling, and our spatial heatmap as the input to the spatial encoding layer.

	Baseline	Gau. Noise	Non-Hie	Hie
FID $\downarrow$	8.36	8.31	7.29	**6.81**
DI $\downarrow$	3.64	3.67	2.70	**2.39**

Table 4. **Ablation study on spatial encoding.** We flatten the spatial heatmap and incorporate the vectorized one into latent code, denoted as 'Flatten'. It destroys the $2D$ space structure, and hence cannot improve over the baseline. Instead, encoding heatmaps in the spatial domain is beneficial. The two variants of SEL show a similar result, where SEL$_{norm}$ is slightly better.

Method	Cat [38]		FFHQ [22]	
	FID $\downarrow$	DI $\downarrow$	FID $\downarrow$	DI $\downarrow$
Baseline	8.36	3.64	3.66	1.62
Flatten	8.63	3.71	3.78	1.63
SEL$_{concat}$	7.02	2.47	3.11	0.90
SEL$_{norm}$	**6.81**	**2.39**	**2.96**	**0.73**

an ablation study on LSUN Cat and FFHQ datasets to test various methods. For example, the first way of feeding the spatial heatmap is to flatten the 2D heatmap as a vector, and then concatenate it with the original latent code. This setting aims at validating whether maintaining 2D structure of spatial heatmap is necessary. Besides, we also use two different SEL modules (*i.e.*, SEL$_{concat}$ and SEL$_{norm}$) mentioned in Sec. 3.1. Their details are available in *Supplementary Material*. For a fair comparison, all the ablation studies use $\mathcal{L}_{align}$.

Tab. 4 presents the results. Apparently, simply feeding the spatial heatmap but without the explicit $2D$ structure leads to no gains compared to the baseline. It might imply that it is challenging to use a vector (like the original latent code) to raise the spatial awareness of the generator. Instead, the proposed SEL module could introduce the substantial improvements, demonstrating the effectiveness of the encoding implementation.

Whether Visual Attention of D is Robust and Consistent? As discussed in Sec. 3.2, the alignment loss ($\mathcal{L}_{align}$) uses the D attention maps to guide G. It assumes the attention map from D is stable enough to serve as a supervision signal and valid over the whole training. To validate the design, we first explore the *robustness* of D.

As shown in the left top of Fig. 7, we add random Gaussian noise to a real image from the LSUN Cat dataset, destroying its texture. As the noise amplitude increasing, we can visually see the noise pattern and the local appearance has been over smoothed. D is still attentive to the original important regions, *e.g.*, the human and cat faces. We then test its response to terrible samples generated by a poorly-trained G, illustrated in the right top of Fig. 7. The samples contain distorted human, cat and background. That is, the visual attention of D is sufficiently robust to the noise perturbation and the generated artifacts. Furthermore, as indicated in the bottom of Fig. 7, we validate whether the visual attention is *consistent* throughout the entire training process. At a very early stage of training, D has already localized the discriminative regions. The focus of such visual attention is consistently maintained till the end of the training. The robustness and consistency property of D attention could successfully provide a support for $\mathcal{L}_{align}$.

5. Discussion

Related Work. Generative adversarial networks (GANs) [13] have shown a great success in many generative tasks, such as synthesising photorealistic images. It aims to recover the target distribution via a minimax two-player game, whose global optimum exists as a Nash Equilibrium [10, 13, 16, 17]. Researchers have developed numerous techniques to improve the synthesis quality of GANs, through a Laplacian pyramid framework [8], an all-convolutional deep neural network [28], progressive training [20], spectral normalization [25, 39], and large-sacle GAN training [4, 9]. Recently, the style-based architecture StyleGAN [22] and StyleGAN2 [23] have become the state-of-the-art method for image synthesis, by separating high-level attributes. Besides, some methods also incorporate additional information into discriminator or generator, such as pixel-wise representation [29], 3D pose [26], or neighboring instances [6].

In the early development stage, some methods study the equilibrium between G and D to stabilize training and enhance the synthesis quality [2, 3, 10]. However, the equilibrium problem seems to be neglected in recent years, possibly covered up by the great success in other aspects like the architecture design. Instead, we verify that improving GAN equilibrium could lead to a substantial performance gain, even on the state-of-the-art method StyleGAN2.

Limitation. Though simple and effective, our EqGAN-SA is heuristic and built upon existing techniques. In addition, we notice the spatial encoding operation would sometimes lead to a synthesis blurring at the location of heatmaps boundaries. We consider EqGAN-SA as an empirical study to show that the asymmetry between the spatial awareness of G and D is a source of the GAN
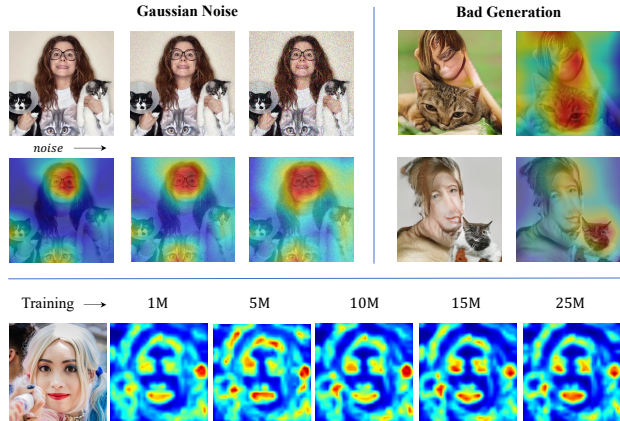

Figure 7. **Robustness and Consistency.** We test the response of D to noisy images and bad generation samples in the top. The bottom visualizes that the D's attention is consistent over the training.

disequilibrium. We hope this work can inspire more works of revisiting the GAN equilibrium and develop more novel methods to improve the image synthesis quality through maneuvering the GAN equilibrium. We will also conduct more theoretical investigation on this issue in the future work.

Ethical Consideration. This paper focuses on studying the disequilibrium of GANs to improve the image synthesis quality. Although only using the public datasets for research and follow their licences, the abuse of our method may bring negative impacts through deep fake generation. Such risks would increase as the synthesis results of GANs are becoming more and more realistic. From the perspective of academia, these risks may be mitigated by promoting the research on deep fake detection. It also requires the management on the models trained with sensitive data.

6. Conclusion

In this paper we explore the problem of GAN equilibrium, and identify one of its possible attributing sources is the information asymmetry between G and D. Specifically, we notice that D spontaneously learns its visual attention while G is not aware of which spatial regions to focus on for a particular synthesis. Therefore, we propose a new training technique EqGAN-SA to reduce such information asymmetry, by enabling spatial awareness of G and aligning it with the attention of D. Qualitative results show that our method successfully makes G to concentrate on specific regions. Experiments on various datasets validate that our method mitigates the disequilibrium in GAN training and substantially improves the overall image synthesis quality. The resulting model with spatial awareness also enables the interactive manipulation of the output image.

References

[1] Youssef Alami Mejjati, Christian Richardt, James Tompkin, Darren Cosker, and Kwang In Kim. Unsupervised attention-guided image-to-image translation. In *Adv. Neural Inform. Process. Syst.*, 2018.

[2] Martin Arjovsky, Soumith Chintala, and Léon Bottou. Wasserstein generative adversarial networks. In *Int. Conf. Mach. Learn.*, pages 214–223, 2017. 1, 2, 7, 8

[3] David Berthelot, Thomas Schumm, and Luke Metz. Began: Boundary equilibrium generative adversarial networks. *arXiv preprint arXiv:1703.10717*, 2017. 8

[4] Andrew Brock, Jeff Donahue, and Karen Simonyan. Large scale gan training for high fidelity natural image synthesis. In *Int. Conf. Learn. Represent.*, 2019. 1, 2, 8

[5] Marisa Carrasco. How visual spatial attention alters perception. *Cognitive processing*, pages 77–88, 2018.

[6] Arantxa Casanova, Marlène Careil, Jakob Verbeek, Michal Drozdzal, and Adriana Romero Soriano. Instance-conditioned gan. In *Adv. Neural Inform. Process. Syst.*, 2021. 8

[7] Xinyuan Chen, Chang Xu, Xiaokang Yang, and Dacheng Tao. Attention-gan for object transfiguration in wild images. In *Eur. Conf. Comput. Vis.*, 2018.

[8] Emily L Denton, Soumith Chintala, Arthur Szlam, and Rob Fergus. Deep generative image models using a laplacian pyramid of adversarial networks. In *Adv. Neural Inform. Process. Syst.*, 2015. 8

[9] Jeff Donahue and Karen Simonyan. Large scale adversarial representation learning. In *Adv. Neural Inform. Process. Syst.*, 2019. 2, 8

[10] William Fedus, Mihaela Rosca, Balaji Lakshminarayanan, Andrew M Dai, Shakir Mohamed, and Ian Goodfellow. Many paths to equilibrium: Gans do not need to decrease a divergence at every step. In *Int. Conf. Learn. Represent.*, 2018. 8

[11] Xavier Glorot, Antoine Bordes, and Yoshua Bengio. Deep sparse rectifier neural networks. In *Proceedings of the fourteenth international conference on artificial intelligence and statistics*, pages 315–323, 2011. 3

[12] Lore Goetschalckx, Alex Andonian, Aude Oliva, and Phillip Isola. Ganalyze: Toward visual definitions of cognitive image properties. In *Int. Conf. Comput. Vis.*, pages 5744–5753, 2019.

[13] Ian Goodfellow, Jean Pouget-Abadie, Mehdi Mirza, Bing Xu, David Warde-Farley, Sherjil Ozair, Aaron Courville, and Yoshua Bengio. Generative adversarial nets. In *Adv. Neural Inform. Process. Syst.*, 2014. 1, 2, 8

[14] Erik Härkönen, Aaron Hertzmann, Jaakko Lehtinen, and Sylvain Paris. Ganspace: Discovering interpretable gan controls. In *Adv. Neural Inform. Process. Syst.*, pages 9841–9850, 2020.

[15] Xingzhe He, Bastian Wandt, and Helge Rhodin. Latentkeypointgan: Controlling gans via latent keypoints. *arXiv preprint arXiv:2103.15812*, 2021.

[16] Martin Heusel, Hubert Ramsauer, Thomas Unterthiner, Bernhard Nessler, and Sepp Hochreiter. Gans trained by a two time-scale update rule converge to a local nash equilibrium. In *Adv. Neural Inform. Process. Syst.*, 2017. 2, 6, 8

[17] Ya-Ping Hsieh, Chen Liu, and Volkan Cevher. Finding mixed Nash equilibria of generative adversarial networks. In *Int. Conf. Mach. Learn.*, volume 97, pages 2810–2819, 2019. 8

[18] Xun Huang and Serge Belongie. Arbitrary style transfer in real-time with adaptive instance normalization. In *Int. Conf. Comput. Vis.*, pages 1501–1510, 2017. 4

[19] Yifan Jiang, Shiyu Chang, and Zhangyang Wang. Transgan: Two pure transformers can make one strong gan, and that can scale up. In *Adv. Neural Inform. Process. Syst.*, 2021.

[20] Tero Karras, Timo Aila, Samuli Laine, and Jaakko Lehtinen. Progressive growing of gans for improved quality, stability, and variation. In *Int. Conf. Learn. Represent.*, 2018. 8

[21] Tero Karras, Miika Aittala, Janne Hellsten, Samuli Laine, Jaakko Lehtinen, and Timo Aila. Training generative adversarial networks with limited data. In *Adv. Neural Inform. Process. Syst.*, pages 12104–12114, 2020. 1, 4, 5

[22] Tero Karras, Samuli Laine, and Timo Aila. A style-based generator architecture for generative adversarial networks. In *IEEE Conf. Comput. Vis. Pattern Recog.*, pages 4401–4410, 2019. 1, 2, 4, 7, 8

[23] Tero Karras, Samuli Laine, Miika Aittala, Janne Hellsten, Jaakko Lehtinen, and Timo Aila. Analyzing and improving the image quality of stylegan. In *IEEE Conf. Comput. Vis. Pattern Recog.*, pages 8110–8119, 2020. 1, 2, 5, 8

[24] Alex Krizhevsky, Geoffrey Hinton, et al. Learning multiple layers of features from tiny images. 2009. 7

[25] Takeru Miyato, Toshiki Kataoka, Masanori Koyama, and Yuichi Yoshida. Spectral normalization for generative adversarial networks. In *Int. Conf. Learn. Represent.*, 2018. 7, 8

[26] Michael Niemeyer and Andreas Geiger. Giraffe: Representing scenes as compositional generative neural feature fields. In *IEEE Conf. Comput. Vis. Pattern Recog.*, 2021. 8

[27] Taesung Park, Ming-Yu Liu, Ting-Chun Wang, and Jun-Yan Zhu. Semantic image synthesis with spatially-adaptive normalization. In *IEEE Conf. Comput. Vis. Pattern Recog.*, pages 2337–2346, 2019. 4

[28] Alec Radford, Luke Metz, and Soumith Chintala. Unsupervised representation learning with deep convolutional generative adversarial networks. In *Int. Conf. Learn. Represent.*, 2016. 1, 7, 8

[29] Edgar Schonfeld, Bernt Schiele, and Anna Khoreva. A u-net based discriminator for generative adversarial networks. In *IEEE Conf. Comput. Vis. Pattern Recog.*, 2020. 8

[30] Ramprasaath R Selvaraju, Michael Cogswell, Abhishek Das, Ramakrishna Vedantam, Devi Parikh, and Dhruv Batra. Grad-cam: Visual explanations from deep networks via gradient-based localization. In *Int. Conf. Comput. Vis.*, pages 618–626, 2017. 1, 2

[31] Yujun Shen, Jinjin Gu, Xiaoou Tang, and Bolei Zhou. Interpreting the latent space of gans for semantic face editing. In *IEEE Conf. Comput. Vis. Pattern Recog.*, 2020.

[32] Yujun Shen and Bolei Zhou. Closed-form factorization of latent semantics in gans. In *IEEE Conf. Comput. Vis. Pattern Recog.*, 2021.

[33] Timo Aila Tero Karras, Samuli Laine. Flickr-faces-hq dataset (ffhq). 4

[34] Andrey Voynov and Artem Babenko. Unsupervised discovery of interpretable directions in the gan latent space. In *Int. Conf. Mach. Learn.*, pages 9786–9796, 2020.

[35] Ting-Chun Wang, Ming-Yu Liu, Jun-Yan Zhu, Andrew Tao, Jan Kautz, and Bryan Catanzaro. High-resolution image synthesis and semantic manipulation with conditional gans. In *IEEE Conf. Comput. Vis. Pattern Recog.*, pages 8798–8807, 2018.

[36] Ceyuan Yang, Yujun Shen, and Bolei Zhou. Semantic hierarchy emerges in deep generative representations for scene synthesis. *Int. J. Comput. Vis.*, 2021. 2, 4

[37] Ceyuan Yang, Yujun Shen, and Bolei Zhou. Semantic hierarchy emerges in deep generative representations for scene synthesis. *Int. J. Comput. Vis.*, pages 1451–1466, 2021.

[38] Fisher Yu, Ari Seff, Yinda Zhang, Shuran Song, Thomas Funkhouser, and Jianxiong Xiao. Lsun: Construction of a large-scale image dataset using deep learning with humans in the loop. *arXiv preprint arXiv:1506.03365*, 2015. 2, 4, 7

[39] Han Zhang, Ian Goodfellow, Dimitris Metaxas, and Augustus Odena. Self-attention generative adversarial networks. In *Int. Conf. Mach. Learn.*, pages 7354–7363, 2019. 8

[40] Bolei Zhou, Aditya Khosla, Agata Lapedriza, Aude Oliva, and Antonio Torralba. Learning deep features for discriminative localization. In *IEEE Conf. Comput. Vis. Pattern Recog.*, pages 2921–2929, 2016. 2